Published in final edited form as:
Chem Biol Interact. 2011 May 30; 191(1-3): 261–268. doi:10.1016/j.cbi.2010.12.017.

Roles of rat and human aldo-keto reductases in metabolism of farnesol and geranylgeraniol

Satoshi Endo[a,b,*], **Toshiyuki Matsunaga**[a], **Chisato Ohta**[a], **Midori Soda**[a], **Ayano Kanamori**[a], **Yukio Kitade**[b], **Satoshi Ohno**[c], **Kazuo Tajima**[d], **Ossama El-Kabbani**[e], and **Akira Hara**[a]

[a]Gifu Pharmaceutical University, Gifu 501-1196, Japan

[b]United Graduate School of Drug Discovery and Medical Information Sciences, Gifu University, Gifu 501-1193, Japan

[c]Faculty of Engineering, Gifu University, Gifu 501-1193, Japan

[d]Hokuriku University, Kanazawa 920-1181, Japan

[e]Monash Institute of Pharmaceutical Sciences, Victoria 3052, Australia

Abstract

Farnesol (FOH) and geranylgeraniol (GGOH) with multiple biological actions are produced from the mevalonate pathway, and catabolized into farnesoic acid and geranylgeranoic acid, respectively, via the aldehyde intermediates (farnesal and geranylgeranial). We investigated the intracellular distribution, sequences and properties of the oxidoreductases responsible for the metabolic steps in rat tissues. The oxidation of FOH and GGOH into their aldehyde intermediates were mainly mediated by alcohol dehydrogenases 1 (in the liver and colon) and 7 (in the stomach and lung), and the subsequent step into the carboxylic acids was catalyzed by a microsomal aldehyde dehydrogenase. In addition, high reductase activity catalyzing the aldehyde intermediates into FOH (or GGOH) was detected in the cytosols of the extra-hepatic tissues, where the major reductase was identified as aldo-keto reductase (AKR) 1C15. Human reductases with similar specificity were identified as AKR1B10 and AKR1C3, which most efficiently reduced farnesal and geranylgeranial among seven enzymes in the AKR1A-1C subfamilies. The overall metabolism from FOH to farnesoic acid in cultured cells was significantly decreased by overexpression of AKR1C15, and increased by addition of AKR1C3 inhibitors, tolfenamic acid and *R*-flurbiprofen. Thus, AKRs (1C15 in rats, and 1B10 and 1C3 in humans) may play an important role in controlling the bioavailability of FOH and GGOH.

Keywords

Alcohol dehydrogenase; Aldehyde dehydrogenase; AKR1C15; AKR1C3; Farnesol; Geranylgeranio

*Corresponding author: Laboratory of Biochemistry, Gifu Pharmaceutical University, 5-6-1 Daigaku-Nishi, Gifu 501-1196, Japan. sendo@gifu-pu.ac.jp .

Conflicts of Interest

The authors declare that there are no conflicts of interest.

1. Introduction

Isoprenoids are intermediates of the mevalonate pathway that produces cholesterol, ubiquinone, dolichol, heme a, and the 15-carbon farnesyl and 20-carbon geranylgeranyl groups of prenylated proteins [1-3]. Prenylation, a post-translational addition of the isoprenyl moieties to proteins from farnesyl pyrophosphate and geranylgeranyl pyrophosphate, has been shown to be crucial for the biological functions of prenylated proteins in the regulation of cell proliferation, differentiation, apoptosis and cytoskeleton organization.

Farnesol (FOH) and geranylgeraniol (GGOH) are produced by dephosphorylation of farnesyl pyrophosphate and geranylgeranyl pyrophosphate, respectively, although they are in turn phosphorylated to their pyrophosphates [3-5]. The two isoprenoids are increasingly known to display multiple functions. FOH was shown to exhibit diverse biological actions such as inhibition of Ca^{2+}-channels [6] and activation of farnesoid X receptor [3], constitutive androstane receptor [7] and peroxisome proliferator-activated receptors α and γ [8]. GGOH was shown to be a ligand for peroxisome proliferator-activated receptors α and γ [8] and a negative regulator of liver X receptor α [9], and its constant synthesis in mouse brain was suggested to be essential for learning [10].

FOH is oxidized into farnesal (FAL), which is then metabolized into farnesoic acid (FA) and prenyl dicarboxylic acids [11,12]. Since no biological action has been found for the metabolites, this metabolism is thought to be a catabolic pathway (Fig. 1). Horse and human alcohol dehydrogenases (ADHs) catalyze the oxidation of FOH [13,14], but the enzyme responsible for the oxidation of FAL into FA remains unknown. GGOH is also converted into geranylgeranoic acid (GGA) and 2,3-dihydrogeranylgeranoic acid via geranylgeranial (GGAL) in rat cultured cells [15]. Distinct from the FOH metabolites, the two carboxylic acid metabolites of GGOH exhibit biological actions, such as induction of apoptosis in hepatoma cells [16], differentiation of mouse osteoblasts [17], and formation of lipid droplets in HL-60 cells [18]. However, there has been no report on the enzymes responsible for the metabolism of GGOH into its metabolites.

Recently, a lysosomal prenylcysteine lyase that releases FAL and GGAL from prenylated proteins was identified, indicating another metabolic pathway that provides the two aldehyde metabolites [19,20]. In addition, FAL was reported to be efficiently reduced by AKR1C15, a rat NADPH-dependent reductase belonging to the aldo-keto reductase (AKR) superfamily [21], proposing the presence of a novel metabolic pathway by which FAL is salvaged into the biologically active FOH. However, it remains unknown whether AKR1C15 reduces GGAL, and how the salvage pathway contributes to the metabolism of FOH and GGOH. In order to identify the enzymes in the catabolism and proposed salvage pathway of FOH and GGOH, we investigated their intracellular distribution, amounts and properties in rat tissues and cultured cells. In this paper, we designate the enzymes in the metabolic steps (Fig. 1) as FOH dehydrogenase (FOH-DH), GGOH dehydrogenase (GGOH-DH), FAL dehydrogenase (FAL-DH), GGAL dehydrogenase (GGAL-DH), FAL reductase (FAL-R) and GGAL reductase (GGAL-R). The results show the importance of the salvage pathway mediated by FAL-R and GGAL-R for controlling the concentrations of FOH and GGOH, and reveal that AKR1C15 is the major enzyme exhibiting both FAL-R and GGAL-R activities in rat extra-hepatic tissues. Therefore, we also examined human enzymes that mediate the salvage pathway.

2. Materials and methods

2.1. Chemicals

All-*trans*-forms of FOH, FAL, GGOH and GGA were purchased from Sigma-Aldrich, Fluka, Wako Chemicals (Osaka, Japan) and Biomol, respectively. *trans,trans*-GGAL was synthesized from GGOH as described previously [22]. *trans,trans*-FA was prepared by incubation of 0.1 mM FAL with 2 units (U) baker's yeast aldehyde dehydrogenase (ALDH, Sigma-Aldrich) in 0.1 M potassium phosphate buffer, pH 8.0, containing 2 mM NAD^+ at 25°C for 12 h. [1-^{14}C] *trans,trans*-GGOH and [1-^{14}C] *trans,trans*-FOH were obtained from American Radiolabeled Chemicals (St. Louis, MO), and resins for column chromatography were from GE Healthcare. An AKR1C1 inhibitor, 3-bromo-5-phenylsalicylic acid, was synthesized as described [23]. All other chemicals were of the highest grade that could be obtained commercially.

2.1. Assay of enzyme activity

Dehydrogenase activity was assayed by measuring the rate of change in NADH absorbance (at 340 nm) or its fluorescence (at 455 nm with an excitation wavelength of 340 nm) in a 2.0-ml reaction mixture containing 0.1 M potassium phosphate, pH 7.4, 2 mM NAD^+, substrate and enzyme. The activities of ADH, FOH-DH, GGOH-DH, FAL-DH and GGAL-DH were determined with 40 mM ethanol, 0.1 mM FOH, 50 μM GGOH, 50 μM FAL and 20 μM GGAL, respectively, as the substrates. In the assay of FAL-R and GGAL-R activities, 0.1 mM NADPH and 50 μM FAL or 20 μM GGAL were used as the coenzyme and substrate, respectively, in the above reaction mixture, and the rate of NADPH oxidation was spectrophotometrically determined. The dehydrogenase and reductase rates were corrected for the non-enzymatic NAD^+ reduction and NADPH oxidation, respectively, by the enzyme samples in the reaction mixture without the substrate. One unit (U) of enzyme activity was defined as the enzyme amount that catalyzes the formation or oxidation of 1 μmol of NAD(P)H per min at 25°C. The apparent K_m and V_{max} values were determined using five concentrations of the substrates by fitting the initial velocities to the Michaelis-Menten equation, and the k_{cat} values were calculated from the V_{max} values assuming the molecular masses of ADH subunit and AKRs as 40 and 36 kDa, respectively. Kinetic constants and IC_{50} values are expressed as the means of two or three determinations.

2.3. Product identification

The reaction was conducted in a 2.0-ml system containing 1 mM NADPH or 2 mM NAD^+, substrate (50 μM FAL, 20 μM GGAL, 50 μM GGOH or 0.1 mM FOH), enzyme and 0.1 M potassium phosphate, pH 7.4. The substrate and products were extracted into 4 volumes of ethyl acetate after 30 min-incubation at 37°C, and were analyzed by TLC as described previously [24].

2.4. Preparation of tissue samples and gel filtration

Tissues were excised from 16-20 week-old female Wistar rats. The livers, lungs and stomachs (each 4 g) were homogenized with 9 volumes of 20 mM Tris-HCl, pH 7.5, containing 0.25 M sucrose, and the homogenates were centrifuged at 700 x *g* for 10 min. The mitochondrial, microsomal and cytosolic fractions were prepared from the supernatants by differential centrifugation, and the proteins of the mitochondrial and microsomal fractions were solubilized as described previously [25]. In the gel-filtration analysis, the extracts of the rat tissues (10 g) were prepared by the centrifugation of the homogenates at 9000 x *g* for 10 min, and subjected to ammonium sulfate fractionation (30-80% saturation). The precipitated proteins were dissolved into 10 ml of buffer A (10 mM Tris-HCl, pH 8.0, plus 2 mM 2-mercaptoethanol), and applied to a Sephadex G-100 column (3 × 90 cm) that

has been equilibrated with the same buffer. The FAL-R and GGAL-R activities in the fractions were determined with 0.1 M potassium phosphate, pH 6.0, containing 1.0 mM 4-methylpyrazole as the assay buffer to eliminate the reductase activity due to ADH. The fractions with FOH/GGOH-DH and FAL/GGAL-R activities were separately pooled and concentrated by ultrafiltration. All procedures including homogenization and gel filtration were carried out at 4°C. Protein concentration was determined by a bicinchoninic acid protein assay reagent kit (Pierce) using bovine serum albumin as the standard.

2.5. cDNA isolation

The cDNAs for ADH1 and ADH7 were isolated from the total RNA preparations of rat liver and stomach, respectively, by reverse transcription (RT)-PCR. The DNA techniques followed the standard procedures described by Sambrook et al. [26]. PCR was performed with *Pfu* DNA polymerase (Stratagene) and the following pairs of sense and antisense primers: 5′-atgagcacagctggaaaagta-3′ and 5′-catgaatgccttcccggttt-3′ for ADH1 cDNA; and 5′-atggacactgctggaaaag-3′ and 5′-cagctctctggatctcaaa-3′ for ADH7 cDNA. The PCR products were ligated into pCR T7/CT-TOPO vectors (Invitrogen), and the expression constructs were transfected into *Escherichia coli* BL21 (DE3) pLysS (Invitrogen). The inserts of the cloned cDNAs were sequenced by using a Beckman CEQ2000XL DNA sequencer.

2.6. Enzyme purification

The recombinant ADH1 and ADH7 were expressed in the *E. coli* cells, which were cultured in a LB medium containing ampicillin (50 μg/mL) for 24 h at 20°C after the addition of 1 mM isopropyl-β-D-thiogalactopyranoside. The enzymes were purified at 4°C from the extracts of the *E. coli* cells, which were obtained by centrifugation (at 12000 x *g* for 15 min) after sonication. In the purification of ADH1, the cell extract was dialyzed against buffer B (10 mM Tris-HCl, pH 8.5, plus 5 mM 2-mercaptoethanol), and applied to a Q-Sepharose column (2 × 20 cm). The enzyme, eluted in the non-adsorbed fraction, was applied to a Blue-Sepharose column (2 × 10 cm). The enzyme was eluted with a linear gradient of 0–0.1 M NaCl in buffer A containing 1 mM NAD^+. The enzyme fractions were concentrated by ultrafiltration, and gel-filtrated on a Sephadex G-200 column (3 × 90 cm) that had been equilibrated with buffer A. The obtained enzyme showed a single 40-kDa protein band on SDS-PAGE analysis. In the purification of ADH7, the cell extract was applied to a DEAE-Sephacel column (2 × 20 cm) after dialysis against buffer C (10 mM Tris-HCl, pH 8.0, plus 5 mM 2-mercaptoethanol). The enzyme was eluted from the column with a linear gradient of 0–0.15 M NaCl in buffer C. The enzyme fraction was applied to the Blue-Sepharose column, and the adsorbed enzyme was eluted with buffer C containing 1 mM NAD^+. The homogeneous preparation of ADH7 was obtained by gel-filtration on the Sephadex G-200 column. Recombinant rat AKRs (1C9 and 1C15) [21,27] and human AKRs (1A1, 1B1 [28], 1B10 [24], 1C1, 1C4 [29], 1C2 [30] and 1C3 [31]) were expressed from their cDNAs, and purified to homogeneity (judged by SDS-PAGE) as described.

The FOH-DHs of rat liver and stomach were purified from the high-molecular weight (MW) enzyme fractions in the gel filtration analyses of the two tissue extracts, according to the procedures for purification of recombinant ADH1 and ADH7, respectively. The hepatic FAL-R was purified from the low-MW enzyme fraction in the gel filtration analysis of the tissue extract. The fraction was dialyzed against buffer D (10 mM Tris-HCl, pH 8.0, containing 5 mM 2-mercaptoethanol and 20% glycerol), and applied to a Q-Sepharose column (2 × 10 cm). The enzyme was eluted with a linear gradient of 0 – 0.1 M NaCl in buffer D, and applied to a Red-Sepharose column (1.2 × 5 cm). The adsorbed enzyme was eluted from the column with buffer D containing 0.5 mM $NADP^+$.

2.7. Mass spectrometry

The identity of the purified enzyme with known ADH or AKR activities was examined by the mass spectrometry method. The purified protein (0.1 mg) was digested by lysylendopeptidase or trypsin, and then the digest was analyzed using a Bruker-Franzen Mass Spectrometry System Ultraflex TOF/TOF with a saturated α-cyano-4-hydroxycinnamic acid matrix as described previously [32].

2.8. RT-PCR analysis

The total RNA samples were prepared from rat tissues and cultured cells, and RT-PCR was carried out using *Taq* DNA polymerase (Takara, Kusazu, Japan) and the gene-specific primers for ADH1 and ADH7 as described above. The cDNA for ALDH3A2 was amplified using sense and antisense primers, 5′-atggagcgacaggtccaacg-3′ and 5′-gtttcctgtgtagagaatgtg-3′. The RT-PCR analyses for the expression of mRNAs for AKR1C15 [21] and AKR1C9 [27] were carried out as described previously.

2.9. Immunochemical experiments

Antibodies against the purified recombinant ADH7 and AKR1C3 were raised in rabbits, and their immunoglobulin fractions were prepared from the antiserum. Immunoprecipitation of ADH7 and AKR1C15 from preparations of purified enzymes and cell extracts using the antibodies against ADH7 and AKR1C15 were performed as described previously [21]. In Western blotting analyses using these antibodies, the immunoreactive proteins were visualized using an enhanced chemi-luminescence substrate system (GE Healthcare).

2.10. Cell culture experiments

Rat gastric mucosa RGM1 cells (RIKEN Cell Bank, Tsukuba, Japan) were cultured in Dulbecco's modified Eagle's medium/Ham's F12 (1 : 1) combined medium supplemented with 10% (v/v) fetal bovine serum, penicillin (100 U/ml), and streptomycin (0.1 mg/ml) at 37°C in a humidified incubator containing 5% CO_2. HeLa and MCF7 cells (ATCC, Manassas, VA) were cultured in Dulbecco's modified Eagle's medium plus 10% fetal bovine serum and the antibiotics. The transfection of the anti-ADH7 antibodies (10 μg/ml of the medium) into the cells was performed with a protein transfection reagent, Profect P-2 (Targeting systems, Santee, CA), according to the manufacturer's manual. The transfected cells were maintained in the medium for 24 h, and then used for experiments.

The pGW1 expression vectors harboring the cDNAs for AKR1B10 and AKR1C15 were constructed as described [24,33]. Similarly, the expression vector harboring the cDNA for AKR1C3 was prepared. The cDNA was initially amplified from the bacterial expression vectors [31] by PCR using the primers. The sense primer, 5′-tt*gaattc*GCCACCatggattccaaacagcagtgt-3′, contains an *Eco*RI site, a Kozak sequence and a start codon, which are shown in italic, capital and underlined letters, respectively. The antisense primer, 5′-cc*ggatcc*ttaatattcatctgaatatggat-3′, is complementary to the bacterial expression vector containing a *Bam*HI site, which is shown in italic letters. After the sequences of the PCR products were verified, they were subcloned at the *Eco*RI and *Bam*HI sites of the pGW1 expression vector. Using a Lipofectamine 2000 Reagent (Invitrogen), the cells were transfected with the expression plasmids. The transfected cells were maintained in the medium containing 2% fetal bovine serum for 24 h, and then used for experiments. The metabolism of GGOH and FOH were initiated by the addition of 1 μM [^{14}C] GGOH and 20 μM [^{14}C] FOH (each 1100 Bq), respectively, to the medium of 90% confluent cells. A portion of the medium was taken at different times, and finally the cells were collected and homogenized. GGOH, FOH and their metabolites in the media and cell homogenates were

extracted into ethyl acetate, analyzed by TLC, and their radioactivities were determined as described previously [24].

3. Results and discussion

3.1. Intracellular distribution of oxidoreductases for isoprenoid alcohols and aldehydes

When the intracellular distribution of the activities of the NAD^+-linked dehydrogenases (FOH-DH, GGOH-DH, FAL-DH and GGAL-DH) and NADPH-linked reductases (FAL-R and GGAL-R) were examined, more than 90% of the total activities of both FOH-DH and GGOH-DH were observed in the cytosolic fractions of the homogenates of rat liver, stomach and lung. In contrast, FAL-DH and GGAL-DH activities were detected only in the microsomal fractions, and FAL-R and GGAL-R activities were recovered only in the cytosolic fractions of the tissue homogenates. The products in the oxidation of FOH, GGOH, FAL and GGAL by the subcellular fractions were identified as FAL, GGAL, FA and GGA, respectively, by TLC, in which their Rf values were identical to the respective standards. Similarly, those in the reduction of FAL and GGAL by the cytosolic fractions were identified as FOH and GGOH, respectively, by TLC analysis. The representative TLC chromatograms of the products formed by the incubation of the substrates with the hepatic subcellular fractions are shown in Supplementary Fig. S1. The specific activities of each enzyme in the cytosolic and microsomal fractions of the tissue homogenates are shown in Table 1. Compared to the extra-hepatic tissues, the liver showed high specific activities of the four enzymes, except that the cytosolic GGAL-R activity was high in the lung. In addition, the activity ratio of cytosolic FOH-DH to GGOH-DH in the liver was 1.8, which was lower than those in the stomach and lung (7 and 11, respectively). The activity ratio of cytosolic FAL-R to GGAL-R in the liver was 6, which is in turn higher than those (approximately 1.5) in the stomach and lung. These differences suggest a possibility that the enzymes responsible for the dehydrogenation of FOH and GGOH and for the reduction of FAL and GGAL are different at least between the liver and the other two tissues. In contrast, the activity ratios of microsomal FAL-DH to GGAL-DH of the three tissues were constant.

3.2. Properties of microsomal FAL-DH and GGAL-DH

More than 90% of the NAD^+-linked FAL-DH and GGAL-DH activities in the microsomal fractions of rat liver, stomach and lung were solubilized by the treatment with 1% Triton X-100 at 4°C for 1 h. Using the solubilized preparation of the hepatic microsomes, the kinetic constants for the substrates, coenzyme requirement and inhibitor sensitivity were examined. The K_m and V_{max} values for FAL were 2.0 μM and 12 mU/mg, respectively, and the respective values for GGAL were 0.7 μM and 4.2 mU/mg. When 2 mM $NADP^+$ was used as the coenzyme, low FAL-DH activity of 2.5 mU/mg was observed. The NAD^+-linked FAL-DH activity was completely inactivated by incubation with 10 μM *p*-chloromercuribenzoate for 5 min at 25°C, and inhibited by chloral hydrate (IC_{50}=28 ± 3 μM) and 4-hydroxyacetophenone (IC_{50}=13 ± 1 μM), which are known inhibitors of rat and human microsomal ALDHs [34,35].

An ALDH isoenzyme and its cDNA have been isolated from rat liver microsomes [36,37], and this is the only microsomal ALDH isoenzyme (ALDH3A2) found in the rat genome database (http://rgd.mcw.edu/). The isoenzyme is also called fatty aldehyde dehydrogenase because of its high affinity towards aliphatic aldehydes of 7-9 carbon chains [36]. The dual coenzyme specificity and inhibitor sensitivity of the present rat microsomal FAL-DH are similar to those reported for rat microsomal ALDH3A2 [33,35], which is ubiquitously expressed in rat tissues [37]. The expression of the mRNA for ALDH3A2 in rat liver, stomach, lung and colon was confirmed by RT-PCR (data not shown). Thus, ALDH3A2

may be the enzyme that catalyzes the oxidation of FAL and GGAL into FA and GGA, respectively.

3.3. Properties of cytosolic FOH-DH and GGOH-DH

In order to examine whether the different enzymes that are responsible for the oxidation of FOH and GGOH depend on rat tissues, we partially purified the cytosolic enzymes in the liver, stomach, lung and colon by gel-filtration on the Sephadex G-100 column (Supplementary Fig. S2). In all analyses of the four tissues, the FOH-DH and GGOH-DH activities were eluted at the same high-MW position (around 80 kDa). The elution patterns were also identical to that of the ethanol dehydrogenase activity, suggesting that the activities of FOH-DH and GGOH-DH are attributed to ADH. As ADH is rich in rat liver, the hepatic high-MW enzyme showed the highest specific activities towards FOH and GGOH (Table 2). However, the activity ratios of FOH-DH to GGOH-DH in the high-MW enzymes were different among the four tissues. The ratio was high for the liver and colon enzymes, whereas it was low for the stomach and lung enzymes. In addition, the liver and colon enzymes showed lower K_m values for ethanol and FOH than the gastric and pulmonary enzymes. Furthermore, a similar difference in sensitivity to 4-methylpyrazole, an ADH inhibitor [38], was observed among the tissue enzymes, although all the tissue enzymes were inhibited to a similar extent by other ADH inhibitors, 1,10-phenanthroline and 13-*cis*-retinoic acid [39].

Three ADH isoenzymes, ADH1, ADH5 and ADH7, have been purified from rat tissues, and differ in their substrate specificity and tissue distribution [38-40]. Among the isoenzymes, ADH1 and ADH7 are highly expressed in the liver and stomach, respectively, and oxidize both ethanol and long-chain aliphatic alcohols. Therefore, we prepared recombinant ADH1 and ADH7, and compared their properties with those of the high-MW FOH-DH and GGOH-DH partially purified from rat tissues (Table 2). With respect to the activity ratios among ethanol, FOH and GGOH, K_m values for the substrates and sensitivity to 4-methylpyrazole, ADH1 resembles the enzymes in the liver and colon, and ADH7 is similar to the enzymes in the stomach and lung. In addition, the lung and stomach enzymes were almost completely immunoprecipitated by the anti-ADH7 antibodies that did not precipitate the hepatic and colonic enzymes and ADH1 (Fig. 2A). When the liver and stomach enzymes were purified to homogeneity and their lysylendopeptidase-digested peptides were analyzed by the mass spectrometry method, the sequence (composed of a total 106 residues) of the liver enzyme and that (composed of a total 225 residues) of the stomach enzyme were identical to those deduced from the cDNAs for ADH1 and ADH7, respectively. These results clearly indicate that the oxidation of FOH and GGOH in the rat tissues is predominantly catalyzed by the two tissue-specific ADH isoenzymes. The k_{cat}/K_m values for GGOH of ADH1 and ADH7 were 90 and 150 $min^{-1}\mu M^{-1}$, respectively, which are higher than the values of the two isoenzymes for FOH (34 and 67 $min^{-1}\mu M^{-1}$, respectively). Although the FOH-DH activity of horse and human ADHs have been reported [13,14], this study demonstrates for the first time that ADH efficiently oxidizes GGOH.

To further confirm the oxidation of GGOH into GGAL by the tissue-specific ADH isoenzymes and involvement of the microsomal ALDH3A2 in the subsequent metabolism into GGA, we investigated the metabolism of GGOH in the gastric mucosa RGM1 cells, in which the expression of the mRNAs for ADH7 and ALDH3A2, but not that for ADH1, were confirmed by RT-PCR (data not shown). GGOH was metabolized into GGA (Fig. 2B), which accumulated in the medium proportionally with the decrease in GGOH (Fig. 2C), indicating that the metabolized GGA is excreted from the cells. While unknown metabolites with high R_f values were observed in the cells, GGAL was not detected in both medium and cells probably because of its rapid metabolism into GGA by ALDH3A2. The metabolic rate from GGOH into GGA was significantly decreased by introducing the anti-ADH7-

antibodies into the cells (Fig. 2C). These results indicate that GGOH is mainly metabolized into GGA via GGAL by ADH7 and ALDH3A2 in the cells, and also support the predominant role of ADH7 in the first step of the GGOH catabolism in rat stomach.

3.4. Properties of cytosolic FAL-R and GGAL-R

In the gel-filtration analysis of the cytosolic proteins in the liver, stomach, lung and colon, the FAL-R and GGAL-R activities were co-eluted at the low-MW fraction, which is distinct from the high-MW FOH-DH activity. The molecular masses of the tissue FAL-R and GGAL-R are similar to that of AKR1C15 (36 kDa) that is known as the only rat enzyme being able to reduce FAL [21]. AKR1C15 reduced GGAL more efficiently than FAL: The K_m and k_{cat}/K_m values for GGAL were of 0.2 μM and 6.0 $min^{-1}μM^{-1}$ respectively, while the respective values for FAL are reported to be 5.6 μM and 2.1 $min^{-1}μM^{-1}$. When the K_m values for the isoprenyl aldehydes were compared among the low-MW reductases from the rat four tissues, the liver enzyme showed higher values for FAL and GGAL (26 and 2.1 μM, respectively) than the enzymes from the stomach, lung and colon. The K_m values of the extra-hepatic enzymes for FAL and GGAL are 6 - 8 μM and 0.2 - 0.5 μM, respectively, which are similar to those of AKR1C15. In addition, the liver enzyme differed from the other tissue enzymes in sensitivity to potent AKR1C15 inhibitors (3′,3″,5′,5″-tetraiodo-phenolphthalein and 3′,3″,5′,5″-tetrabromophenolphthalein) [21]: The two inhibitors (1 μM) showed less than 20% inhibition for the liver enzyme activity, but inhibited more than 80% of the activities of the stomach, lung and colon. The results suggest that the low-MW FAL-R and GGAL-R in the three extra-hepatic tissues are identical to AKR1C15, but other reductase(s) for FAL and GGAL exist in the liver. This was further supported by immunoprecipitation using the anti-AKR1C15 antibody which monospecifically reacts to the antigen [21]. The FAL-R activities from the stomach, lung and colon were decreased by the antibody in a dose-dependent manner, but only 20% of the enzyme activity of the liver was precipitated at high concentrations of the antibody (Fig. 3A). Thus, it is concluded that in the stomach, lung and colon AKR1C15 acts as a predominant reductase for FAL and GGAL.

The above results suggest that in the liver other reductase(s) for the isoprenyl aldehydes may be expressed more than AKR1C15. To identify the major form of the hepatic low-MW reductases for FAL and GGAL, we purified the enzyme to homogeneity from the low-MW fraction obtained by the gel-filtration. The purified enzyme reduced both FAL and GGAL, and showed higher K_m for FAL and GGAL (30 and 3.9 μM, respectively) and lower k_{cat}/K_m values (0.2 and 0.3 $min^{-1}μM^{-1}$, respectively) than AKR1C15. This enzyme also exhibited high reductase activity towards 3-ketosteroids: For example, the K_m and k_{cat} values for 5β-androstane-3,17-dione were 1.6 μM and 25 min^{-1}, respectively. In addition, more than 90% of the FAL-R activity of the purified enzyme was inhibited by 5 μM medroxyprogesterone acetate, 5 μM indomethacin and 50 μM betamethasone, which are inhibitors of AKR1C9, i.e., rat 3α-hydroxysteroid dehydrogenase [41,42]. Furthermore, the sequences (composed of a total 94 residues) of nine tryptic peptides derived from the purified enzyme were identical to those deduced from the cDNA for AKR1C9. Indeed, recombinant AKR1C9 reduced FAL and GGAL and its kinetic constants for the substrates were almost the same as those of the purified liver enzyme. The results clearly indicate that the hepatic FAL-R and GGAL-R activities other than those by AKR1C15 are mostly due to AKR1C9, which is highly expressed in rat liver [43].

The above results demonstrate the presence of the reductases for FAL and GGAL in rat tissues, suggesting that the enzymes play a role in regulation of the metabolic rates from FOH and GGOH to their carboxylic acids by reducing FAL and GGAL back into FOH and GGOH, respectively. In spite of the lower k_{cat} values for FAL and GGAL of AKR1C15 than those for FOH and GGOH of ADH isoenzymes, the gel-filtration analysis indicated that

AKR1C15 is highly expressed in the extra-hepatic tissues. AKR1C15 is a more efficient isoprenyl aldehyde reductase than AKR1C9 *in vitro*, and is expressed in many rat tissues including vascular endothelial cells [21]. Therefore, we further examined the role of AKR1C15 in the metabolism of FOH using the AKR1C15-overexpressing HeLa cells, which were employed because the expression plasmid could not be transfected into rat RGM1 cells. On Western blot analysis using the anti-AKR1C15 antibody, a 36-kDa immunoreactive band was detected only in the transfected HeLa cells, which showed 5-fold higher FAL-R activity (1.9 mU/mg) than the control cells transfected with the vector alone. FOH was rapidly converted into FA in the control cells, in which FA accumulated in the medium and FAL was hardly observed, similarly to the metabolism of GGOH in RGM1 cells. Compared to the control cells, the metabolic rate from FOH to FA was greatly decreased in the AKR1C15-overexpressed cells (Fig. 3B), indicating that AKR1C15 reduces low concentrations of FAL produced from the oxidation of the added FOH. This supports the proposed role of the reductase in controlling the cellular concentrations of FOH and GGOH, which are utilized for sterol synthesis and protein prenylation, and exhibit multiple biological actions [2,3,6-10].

3.5. Human reductases for FAL and GGAL

Considering the role of rat AKRs in regulating the metabolic rates from biologically active FOH and GGOH to their carboxylic acids, it is particularly interesting to identify human enzymes that function as FAL-R and GGAL-R. Human enzymes in the AKR superfamily differ from rodent enzymes in molecular species and properties [44], and four human AKRs (1C1-1C4) belong to the AKR1C subfamily. The kinetic constants of the four AKRs for FAL and GGAL were determined and compared with those of human AKR1B10 and AKR1B1, which are reported to reduce the two isoprenyl aldehydes [24] (Table 3). FAL was most efficiently reduced by AKR1B10, followed by AKR1C3 and AKR1C2. AKR1C3 and AKR1B10 were also excellent reductases towards GGAL. In particular, the K_m value of AKR1C3 for GGAL is lower than those for previously known substrates (steroids and prostaglandins), and its k_{cat}/K_m value is 12-fold higher than that for prostaglandin D_2 which has been recognized as the best endogenous substrate of this enzyme [31,44]. It should be noted that FAL and GGAL were hardly reduced by human carbonyl reductase 1, dicarbonyl-xylulose reductase and dehydrogenase/reductase (SDR family) member 4, which exhibit broad substrate specificity for carbonyl compounds and belong to the short-chain dehydrogenase/reductase superfamily [44].

Since AKR1C3 efficiently reduced FAL and GGAL in vitro, its contribution to cellular metabolism of FAL was examined using MCF7 cells instead of HeLa cells (Fig. 4). RT-PCR analysis revealed that MCF7 cells expressed the mRNAs for AKR1C1, AKR1C2 and AKR1C3 more highly than HeLa cells, although the two cell lines showed no significant expression of the mRNAs for AKR1B10 and AKR1C4 (data not shown). The metabolic rate from FOH to FA (i.e., the amount of FA formed) in MCF7 cells was low compared to that in HeLa cells (i.e., the FA amount in the 6 h-incubated control cells in Fig. 3B). This suggests that AKR1C1, AKR1C2 and/or AKR1C3 act as FAL-R and reduce FAL back to FOH. To test this possibility and identify the major FAL-R species, we examined the effects of inhibitors of human AKRs on the cellular metabolism of FOH. Since nonsteroidal anti-inflammatory drugs have been reported to inhibit human AKRs (1B10, 1C1, 1C2 and 1C3) [45,46,47], we first compared the inhibitory effects of the drugs on the AKRs *in vitro*. AKR1C3 was potently inhibited by several nonsteroidal anti-inflammatory drugs (Table 4), of which tolfenamic acid and *R*-flurbiprofen were most selective to AKR1C3 and showed competitive inhibition with respect to the substrate *S*-(+)-1,2,3,4-tetrahydro-1-naphthol (K_i values were 8 and 610 nM, respectively). Tolfenamic acid and *R*-flurbiprofen increased the formation of FA from FOH in the MCF7 cells in a dose-dependent manner (Fig. 4). In

contrast, no significant changes in the cellular FOH metabolism were observed by the addition of (Z)-2-(4-methoxyphenylimino)-7-hydroxy-N-(pyridin-2-yl)-2H-chromene-3-carboxamide (a potent inhibitor of both AKR1B10 and AKR1B1) [48] and 3-bromo-5-phenylsalicylic acid that is a more potent inhibitior of AKR1C1 than AKR1C2 [23]. The data reveal that AKR1C3 is the major FAL-R in MCF7 cells, and significantly affects the catabolic rate from FOH to FA.

In human cells that highly expresses AKR1C3 like MCF7 cells, the enzyme may also act as GGAL-R because of its high catalytic efficiency for GGAL. In the metabolism of GGOH, the reversible oxidation of GGOH into GGAL by ADH and AKRs may also be the limiting step in the pathway for the synthesis of GGA and 2,3-dihydrogeranylgeranoic acid, which exhibit biological actions on several cultured cells [16,17,18]. AKR1C3 is suggested to be involved in proliferation of breast and prostate cancers through the metabolism of androgen and prostaglandins [49]. AKR1B10, another human enzyme that efficiently reduces FAL and GGAL, is elevated in cancer lesions such as liver and lung cancers, and suggested to be involved in cancer cell proliferation through the metabolism of retinoids and fatty acids [50]. Considering the anticancer action of GGA against human hepatic cancer cells [16], elevated AKR1C3 or AKR1B10 might be responsible for proliferation of the cancer cells by preventing the production of anti-cancerous GGA, as well as by providing GGOH which is the substrate in prenylation of small G-proteins. Further studies in our laboratories are underway to elucidate the human enzymes in the proposed reversible oxidation of the isoprenols and their regulatory functions of human cancerous cells.

Supplementary Material

Refer to Web version on PubMed Central for supplementary material.

Acknowledgments

This work was supported by Grant-in-Aids for young scientists and scientific research from the Japan Society for the Promotion of Science, and by a grant for encouragement of young scientists from Gifu Pharmaceutical University. SE was supported by USPHS NIH grant R13-AA019612 to present this work at the 15th International Meeting on Enzymology and Molecular Biology of Carbonyl Metabolism in Lexington, KY USA.

Appendix

Supplementary data (Fig. S1 and Fig. S2)

Abbreviations

ADH	alcohol dehydrogenase
AKR	aldo-keto reductase
ALDH	aldehyde dehydrogenase
FA	farnesoic acid
FAL	farnesal
FAL-DH	FAL dehydrogenase
FAL-R	FAL reductase
FOH	farnesol
FOH-DH	FOH dehydrogenase

GGA	geranylgeranoic acid
GGAL	geranylgeranial
GGAL-DH	GGAL dehydrogenase
GGAL-R	GGAL reductase
GGOH	geranylgeraniol
GGOH-DH	GGOH dehydrogenase
MW	molecular weight
RT	reverse transcription
U	unit

References

[1]. Goldstein JL, Brown MS. Regulation of the mevalonate pathway. Nature. 1990; 343:425–430. [PubMed: 1967820]

[2]. Edwards PA, Ericsson J. Sterols and isoprenoids: signaling molecules derived from the cholesterol biosynthetic pathway. Annu. Rev. Biochem. 1999; 68:157–185. [PubMed: 10872447]

[3]. Bifulco M. Role of the isoprenoid pathway in ras transforming activity, cytoskeleton organization, cell proliferation and apoptosis. Life Sci. 2005; 77:1740–1749. [PubMed: 15955538]

[4]. Bansal VS, Vaidya S. Characterization of two distinct allyl pyrophosphatase activities from rat liver microsomes. Arch. Biochem. Biophys. 1994; 315:393–399. [PubMed: 7986083]

[5]. Ownby SE, Hohl RJ. Isoprenoid alcohols restore protein isoprenylation in a time-dependent manner independent of protein synthesis. Lipids. 2003; 38:751–759. [PubMed: 14506838]

[6]. Roullet JB, Spaetgens RL, Burlingame T, Feng ZP, Zamponi GW. Modulation of neuronal voltage-gated calcium channels by farnesol. J. Biol. Chem. 1999; 274:25439–25446. [PubMed: 10464274]

[7]. Kocarek TA, Mercer-Haines NA. Squalestatin 1-inducible expression of rat CYP2B: evidence that an endogenous isoprenoid is an activator of the constitutive androstane receptor. Mol. Pharmacol. 2002; 62:1177–1186. [PubMed: 12391282]

[8]. Takahashi N, Kawada T, Goto T, Yamamoto T, Taimatsu A, Matsui N, Kimura K, Saito M, Hosokawa M, Miyashita K, Fushiki T. Dual action of isoprenols from herbal medicines on both PPARγ and PPARα in 3T3-L1 adipocytes and HepG2 hepatocytes. FEBS Lett. 2002; 514:315–322. [PubMed: 11943173]

[9]. Forman BM, Ruan B, Chen J, Schroepfer GJ Jr. Evans RM. The orphan nuclear receptor LXRα is positively and negatively regulated by distinct products of mevalonate metabolism. Proc. Natl. Acad. Sci. U S A. 1997; 94:10588–10593. [PubMed: 9380679]

[10]. Kotti TJ, Ramirez DM, Pfeiffer BE, Huber KM, Russell DW. Brain cholesterol turnover required for geranylgeraniol production and learning in mice. Proc. Natl. Acad. Sci. USA. 2006; 103:3869–3874. [PubMed: 16505352]

[11]. Fliesler SJ, Schroepfer GJ Jr. Metabolism of mevalonic acid in cell-free homogenates of bovine retinas. Formation of novel isoprenoid acids. J. Biol. Chem. 1983; 258:15062–15070. [PubMed: 6654904]

[12]. Gonzalez-Pacanowska D, Arison B, Havel CM, Watson JA. Isoprenoid synthesis in isolated embryonic Drosophila cells. Farnesol catabolism and ω-oxidation. J. Biol. Chem. 1988; 263:1301–1306. [PubMed: 3335546]

[13]. Waller GR. Dehydrogenation of trans-trans farnesol by horse liver alcohol dehydrogenase. Nature. 1965; 207:1389–1390. [PubMed: 5886041]

[14]. Keung WM. Human liver alcohol dehydrogenases catalyze the oxidation of the intermediary alcohols of the shunt pathway of mevalonate metabolism. Biochem. Biophys. Res. Commun. 1991; 174:701–707. [PubMed: 1993065]

[15]. Kodaira Y, Usui K, Kon I, Sagami H. Formation of (R)-2,3-dihydro-geranylgeranoic acid from geranylgeraniol in rat thymocytes. J. Biochem. 2002; 132:327–334. [PubMed: 12153732]

[16]. Shidoji Y, Nakamura N, Moriwaki H, Muto Y. Rapid loss in the mitochondrial membrane potential during geranylgeranoic acid-induced apoptosis. Biochem. Biophys. Res. Commun. 1997; 230:58–63. [PubMed: 9020060]

[17]. Wang X, Wu J, Shidoji Y, Muto Y, Ohishi N, Yagi K, Ikegami S, Shinki T, Udagawa N, Suda T, Ishimi Y. Effects of geranylgeranoic acid in bone: induction of osteoblast differentiation and inhibition of osteoclast formation. J. Bone Miner. Res. 2002; 17:91–100. [PubMed: 11771673]

[18]. Kodaira Y, Kusumoto T, Takahashi T, Matsumura Y, Miyagi Y, Okamoto K, Shidoji Y, Sagami H. Formation of lipid droplets induced by 2,3-dihydrogeranylgeranoic acid distinct from geranylgeranoic acid. Acta Biochim. Pol. 2007; 54:777–782. [PubMed: 18066407]

[19]. Zhang L, Tschantz WR, Casey PJ. Isolation and characterization of a prenylcysteine lyase from bovine brain. J. Biol. Chem. 1997; 272:23354–23359. [PubMed: 9287348]

[20]. Lu JY, Hofmann SL. Thematic review series: lipid posttranslational modifications. Lysosomal metabolism of lipid-modified proteins. J. Lipid Res. 2006; 47:1352–1357. [PubMed: 16627894]

[21]. Endo S, Matsunaga T, Horie K, Tajima K, Bunai Y, Carbone V, El-Kabbani O, Hara A. Enzymatic characteristics of an aldo-keto reductase family protein (AKR1C15) and its localization in rat tissues. Arch. Biochem. Biophys. 2007; 465:136–147. [PubMed: 17574202]

[22]. Doyle MP, Yan M. Attempted synthesis of casbene by intramolecular cyclopropanation. ARKIVOC 2002. 2002:180–185. Part viii.

[23]. El-Kabbani O, Scammells PJ, Gosling J, Dhagat U, Endo S, Matsunaga T, Soda M, Hara A. Structure-guided design, synthesis, and evaluation of salicylic acid-based inhibitors targeting a selectivity pocket in the active site of human 20α-hydroxysteroid dehydrogenase (AKR1C1). J. Med. Chem. 2009; 52:3259–3264. [PubMed: 19397269]

[24]. Endo S, Matsunaga T, Mamiya H, Ohta C, Soda M, Kitade Y, Tajima K, Zhao HT, El-Kabbani O, Hara A. Kinetic studies of AKR1B10, human aldose reductase-like protein: Endogenous substrates and inhibition by steroids. Arch. Biochem. Biophys. 2009; 487:1–9. [PubMed: 19464995]

[25]. Ishikura S, Usami N, Kitahara K, Isaji T, Oda K, Nakagawa J, Hara A. Enzymatic characteristics and subcellular distribution of a short-chain dehydrogenase/reductase family protein, P26h, in hamster testis and epididymis. Biochemistry. 2001; 40:214–224. [PubMed: 11141073]

[26]. Sambrook, J.; Fritsch, EF.; Maniatis, T. Molecular Cloning: A Laboratory Manual. second ed.. Cold Spring Harbor Laboratory; New York: 1989.

[27]. Sanai M, Endo S, Matsunaga T, Ishikura S, Tajima K, El-Kabbani O, Hara A. Rat NAD^+-dependent 3α-hydroxysteroid dehydrogenase (AKR1C17): A member of the aldo-keto reductase family highly expressed in kidney cytosol. Arch. Biochem. Biophys. 2007; 464:122–129. [PubMed: 17475203]

[28]. Iino T, Tabata M, Takikawa S, Sawada H, Shintaku H, Ishikura S, Hara A. Tetrahydrobiopterin is synthesized from 6-pyruvoyl-tetrahydropterin by the human aldo-keto reductase AKR1 family members. Arch. Biochem. Biophys. 2003; 416:180–187. [PubMed: 12893295]

[29]. Matsuura K, Hara A, Deyashiki Y, Iwasa H, Kume T, Ishikura S, Shiraishi H, Katagiri Y. Roles of the C-terminal domains of human dihydrodiol dehydrogenase isoforms in the binding of substrates and modulators: probing with chimaeric enzymes. Biochem. J. 1998; 336:429–436. [PubMed: 9820821]

[30]. Shiraishi H, Ishikura S, Matsuura K, Deyashiki Y, Ninomiya M, Sakai S, Hara A. Sequence of the cDNA of a human dihydrodiol dehydrogenase isoform (AKR1C2) and tissue distribution of its mRNA. Biochem. J. 1998; 334:399–405. [PubMed: 9716498]

[31]. Matsuura K, Shiraishi H, Hara A, Sato K, Deyashiki Y, Ninomiya M, Sakai S. Identification of a principal mRNA species for human 3α-hydroxysteroid dehydrogenase isoform (AKR1C3) that exhibits high prostaglandin D_2 11-ketoreductase activity. J. Biochem. 1998; 124:940–946. [PubMed: 9792917]

[32]. Ohno S, Matsui M, Yokogawa T, Nakamura M, Hosoya T, Hiramatsu T, Suzuki M, Hayashi N, Nishikawa K. Site-selective post-translational modification of proteins using an unnatural amino acid, 3-azidotyrosine. J. Biochem. 2007; 141:335–343. [PubMed: 17202192]

[33]. Matsunaga T, Shinoda Y, Inoue Y, Endo S, El-Kabbani O, Hara A. Protective effect of a rat aldo-keto reductase (AKR1C15) on endothelial cell damage elicited by 4-hydroxy-2-nonenal. Chem. Biol. Interact. submitted as a preceding paper of this paper.

[34]. Lindahl R, Evces S. Rat liver aldehyde dehydrogenase. I. Isolation and characterization of four high Km normal liver Isozymes. J. Biol. Chem. 1984; 259:11986–11990. [PubMed: 6480593]

[35]. Kelson TL, Secor McVoy JR, Rizzo WB. Human liver fatty aldehyde dehydrogenase: microsomal localization, purification, and biochemical characterization. Biochim. Biophys. Acta. 1997; 1335:99–110. [PubMed: 9133646]

[36]. Mitchell DY, Petersen DR. Oxidation of aldehydic products of lipid peroxidation by rat liver microsomal aldehyde Dehydrogenase. Arch. Biochem. Biophys. 1989; 269:11–17. [PubMed: 2916835]

[37]. Miyauchi K, Masaki R, Taketani S, Yamamoto A, Akayama M, Tashiro Y. Molecular cloning, sequencing, and expression of cDNA for rat liver microsomal aldehyde Dehydrogenase. J. Biol. Chem. 1991; 266:19536–19542. [PubMed: 1717467]

[38]. Julià P, Farrés J, Parés X. Characterization of three isoenzymes of rat alcohol dehydrogenase. Tissue distribution and physical and enzymatic properties. Eur. J. Biochem. 1987; 162:179–189. [PubMed: 3816781]

[39]. Allali-Hassani A, Peralba JM, Martras S, Farrés J, Parés X. Retinoids, ω-hydroxyfatty acids and cytotoxic aldehydes as physiological substrates, and H_2-receptor antagonists as pharmacological inhibitors, of human class IV alcohol Dehydrogenase. FEBS Lett. 1998; 426:362–366. [PubMed: 9600267]

[40]. Boleda MD, Saubi N, Farrés J, Parés X. Physiological substrates for rat alcohol dehydrogenase classes: aldehydes of lipid peroxidation, ω-hydroxyfatty acids, and retinoids. Arch. Biochem. Biophys. 1993; 307:85–90. [PubMed: 8239669]

[41]. Sunde A, Rosness PA, Eik-Nes KB. Effects in vitro of medroxyprogesterone acetate on steroid metabolizing enzymes in the rat: selective inhibition of 3α-hydroxysteroid oxidoreductase activity. J. Steroid Biochem. 1982; 17:197–203. [PubMed: 6213817]

[42]. Penning TM, Mukharji I, Barrows S, Talalay P. Purification and properties of a 3α-hydroxysteroid dehydrogenase of rat liver cytosol and its inhibition by anti-inflammatory drugs. Biochem. J. 1984; 222:601–611. [PubMed: 6435601]

[43]. Smithgall TE, Penning TM. Indomethacin-sensitive 3α-hydroxysteroid dehydrogenase in rat tissues. Biochem. Pharmacol. 1985; 34:831–835. [PubMed: 3856432]

[44]. Matsunaga T, Shintani S, Hara A. Multiplicity of mammalian reductases for xenobiotic carbonyl compounds. Drug Metab. Pharmacokinet. 2006; 21:1–18. [PubMed: 16547389]

[45]. Bauman DR, Rudnick SI, Szewczuk LM, Jin Y, Gopishetty S, Penning TM. Development of nonsteroidal anti-inflammatory drug analogs and steroid carboxylates selective for human aldo-keto reductase isoforms: potential antineoplastic agents that work independently of cyclooxygenase isozymes. Mol. Pharmacol. 2005; 67:60–68. [PubMed: 15475569]

[46]. Gobec S, Brozic P, Rizner TL. Nonsteroidal anti-inflammatory drugs and their analogues as inhibitors of aldo-keto reductase AKR1C3: new lead compounds for the development of anticancer agents. Bioorg. Med. Chem. Lett. 2005; 15:5170–5175. [PubMed: 16183274]

[47]. Endo S, Matsunaga T, Kuwata K, Zhao HT, El-Kabbani O, Kitade Y, Hara A. Chromene-3-carboxamide derivatives discovered from virtual screening as potent inhibitors of the tumour maker, AKR1B10. Bioorg. Med. Chem. 2010; 18:2485–2490. [PubMed: 20304656]

[48]. Endo S, Matsunaga T, Soda M, Tajima K, Zhao HT, El-Kabbani O, Hara A. Selective inhibition of the tumor marker AKR1B10 by antiinflammatory N-phenylanthranilic acids and glycyrrhetic acid. Biol. Pharm. Bull. 2010; 33:886–890. [PubMed: 20460771]

[49]. Penning TM, Byrns MC. Steroid hormone transforming aldo-keto reductases and cancer. Ann. N. Y. Acad. Sci. 2009; 1155:33–42. [PubMed: 19250190]

[50]. Liu J, Wen G, Cao D. Aldo-keto reductase family 1 member B1 inhibitors: old drugs with new perspectives. Recent Pat. Anti-cancer Drug Discov. 2009; 4:246–253.

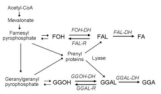

Fig. 1.

Metabolic pathways of FOH and GGOH. Lyase is lysosomal prenylcysteine lyase that releases FAL and GGAL from prenylated proteins, and the other enzymes shown in italic letters are studied in the present work.

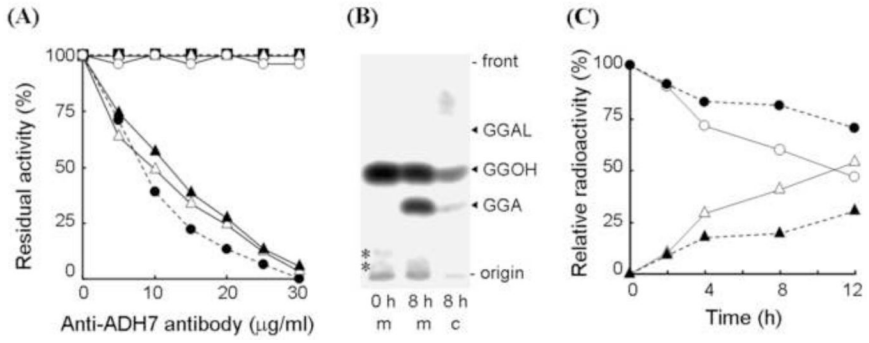

Fig. 2.

Identification of ADH7 as a major enzyme exhibiting FOH-DH and GGOH-DH activities in rat lung, stomach and gastric mucosa RGM1 cells. (A): Immunoprecipitation of FOH-DH activity by the anti-ADH7 antibody. The antibody was incubated with recombinant enzymes (dotted lines), ADH1 (△) and ADH7 (●), and the high-MW enzymes (solid lines) purified from rat liver (■), colon (○), lung (▲) and stomach (△) at 4°C for 12 h. After the immunocomplexes were removed by centrifugation, the activity in the supernatant was determined and is expressed as the percentage of that incubated without the antibody. (B): TLC chromatogram of the metabolites of GGOH in the medium (m) and RGM1 cells (c), which were incubated with 1 μM [^{14}C] GGOH for 0 and 8 h. The positions of authentic samples are shown with arrow heads in the right side. Unknown components present at 0-h culture are shown with asterisks. (C): Effect of transfection of the anti-ADH7 antibody on metabolism of GGOH in RGM1 cells. The cells were cultured 24 h after transfection with the antibody, and then incubated with 1 μM [^{14}C] GGOH. A portion of the medium was taken at indicated times for determination of GGOH (○, ●) and GGA (△,▲) in the non-transfected (open symbols and solid lines) and transfected cells (closed symbols and dotted lines). Relative radioactivities of GGOH and GGA were calculated as described in Materials and methods.

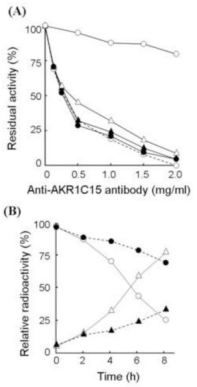

Fig. 3.

Identification of AKR1C15 as a major enzyme exhibiting FAL-R activity in rat tissues. (A): Immunoprecipitation of FAL-R activity by the anti-AKR1C15 antibody. The immunoprecipitation was carried out as described in Fig. 2A. Enzymes are AKR1C15 (○- - -○) and the low-MW enzymes (solid lines) purified from rat liver (○), lung (▲), colon (△), and stomach (●). (B): Effect of the overexpression of AKR1C15 on metabolism of FOH in HeLa cells. The cells were cultured 24 h after transfection with the expression plasmids harboring the cDNA for AKR1C15, and then incubated with 20 μM [^{14}C] FOH. A portion of the medium was taken at indicated times, and the radioactivities of FOH (○, ●) and FA (△,▲) in the media of the control (open symbols and solid lines) and AKR1C15-overexpressed cells (closed symbols and dotted lines) were determined as described in Materials and methods.

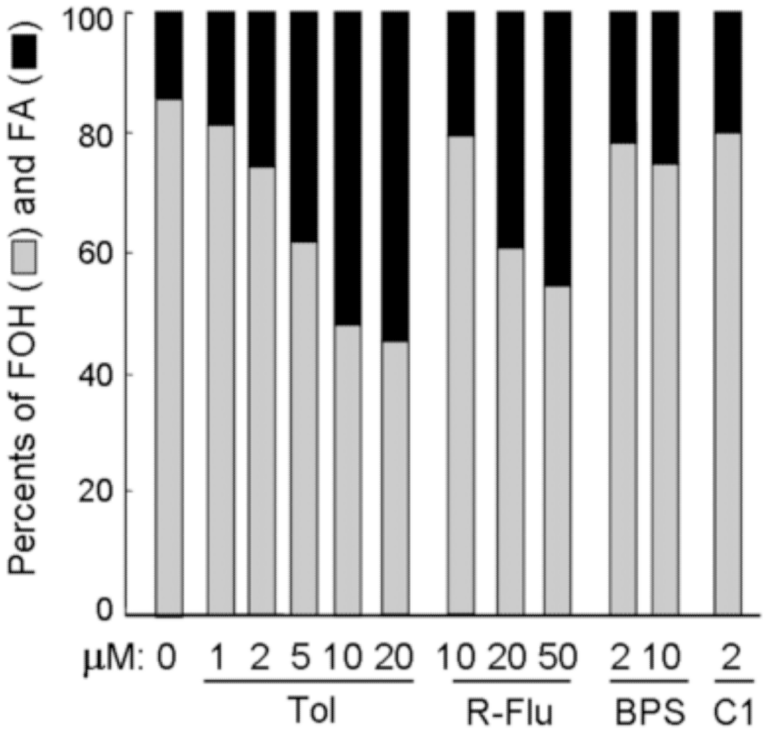

Fig. 4.

Inhibition of FAL reduction in MCF7 cells by selective AKR inhibitors. The cells were incubated for 6 h with 20 μM [^{14}C] FOH in the absence or presence of inhibitors for AKR1C3 (Tol: tolfenamic acid and R-Flu: *R*-flurubiprofen), AKR1C1 (BPS: 3-bromo-5-phenylsalicylic acid) and AKR1B10 (C1: (Z)-2-(4-methoxyphenylimino)-7-hydroxy-N-(pyridin-2-yl)-2H-chromene-3-carboxamide). The radioactivities of FOH and FA in the media of duplicate experiments were measured, and are expressed as the mean percentages, relative to their sum.

Table 1

Activities of FOH-DH, GGOH-DH, FAL-DH, GGAL-DH, FAL-R and GGAL-R in the subcellular fractions of rat liver, stomach and lung

Enzyme	Specific activity (mU/mg)[a]		
	Liver	Stomach	Lung
Cytosolic FOH-DH	18 ± 4	5.4 ± 2.2	2.9 ± 0.3
Cytosolic GGOH-DH	11 ± 3	0.74 ± 0.28	0.26 ± 0.04
Microsomal FAL-DH	11 ± 2	0.84 ± 0.26	0.46 ± 0.06
Microsomal GGAL-DH	3.2 ± 1.1	0.26 ± 0.06	0.10 ± 0.01
Cytosolic FAL-R	8.1 ± 0.5	2.7 ± 0.8	4.0 ± 0.8
Cytosolic GGAL-R	1.3 ± 0.4	1.1 ± 0.2	2.7 ± 0.3

[a]Specific activities of FOH-DH, GGOH-DH, FAL-DH, GGAL-DH, FAL-R and GGAL-R were determined using 0.1 mM FOH, 50 μM GGOH, 50 μM FAL, 20 μM GGAL, 50 μM FAL and 20 μM GGAL, respectively, as the substrates at pH 7.4. The values are means ± S.D. of three rats.

Table 2

Comparison of properties among partially purified FOH-DHs and GGOH-DHs from rat tissues and recombinant ADH1 and ADH7

	Enzyme partially purified from				Recombinant	
	Liver	**Stomach**	**Lung**	**Colon**	**ADH1**	**ADH7**
Activity (U/mg) [a] for						
Ethanol	0.31	0.070	0.014	0.067	0.73	62
FOH	0.29	0.032	0.012	0.054	0.68	43
GGOH	0.20	0.006	0.003	0.022	0.45	3.3
K_m values (μM) [b] for						
Ethanol	570	3400	2900	910	360	3700
FOH	0.7	29	23	1.8	0.8	26
GGOH	0.4	0.8	1.1	0.4	0.2	0.9
IC_{50} (μM) [c] for						
4-Methylpyrazole	2.8	(36%)	(17%)	7.6	5.5	(25%)
1,10-Phenanthroline	30	35	37	36	21	20
13-*cis*-Retinoic acid	12	12	24	7.7	15	15

[a] Dehydrogenase activities for 40 mM ethanol, 0.1 mM FOH and 50 μM GGOH were determined in 0.1 M potassium phosphate, pH 7.4, containing 2 mM NAD^+.

[b] The K_m value represents the mean of three determinations in the above buffer.

[c] The IC_{50} value for the FOH-DH activity was determined and represents the mean of three determinations. The values in the parentheses are the inhibition % by 1 mM inhibitor.

Chem Biol Interact. Author manuscript; available in PMC 2012 May 30.

Table 3

Kinetic constants for FAL and GGAL of human AKRs

AKR	FAL[a]			GGAL[a]		
	K_m (μM)	k_{cat} (min^{-1})	k_{cat}/K_m ($min^{-1}\mu M^{-1}$)	K_m (μM)	k_{cat} (min^{-1})	k_{cat}/K_m ($min^{-1}\mu M^{-1}$)
1A1	60	13	0.22		(0.8) [b]	
1B1	37	27	0.73		(0.3) [b]	
1B10	2.5	23	9.1	0.9	7.5	8.3
1C1	3.1	1.7	0.55		(0.3) [b]	
1C2	1.1	1.8	1.6		(0.4) [b]	
1C3	2.6	2.7	1.1	0.3	3.6	12
1C4	4.7	1.1	0.23	1.1	0.88	0.80

[a]The kinetic constants for FAL and GGAL were determined in 0.1 M potassium phosphate, pH 7.4, containing a saturated concentration (0.1 mM) of NADPH.

[b]The value in parenthesis is calculated from the specific activity with 10 μM GGAL.

Chem Biol Interact. Author manuscript; available in PMC 2012 May 30.

Table 4

Inhibitory effects of non-steroidal anti-inflammatory drugs on human AKRs

Drug	IC_{50} value (μM) [a]						
	AKR 1A1	AKR 1B1	AKR 1B10	AKR 1C1	AKR 1C2	AKR 1C3	AKR 1C4
Tolfenamic acid	30	>100 [b]	>100 [b]	0.71	0.57	0.017	53
Mefenamic acid	28	77	1.6	2.2	2.6	0.11	97
Meclofenamic acid	23	21	12	1.1	2.2	0.43	>100 [b]
R-Flurbiprofen	>50 [b]	35	87	>50 [a]	>50 [a]	1.5	Act [c]
S-Flurbiprofen	>50 [b]	58	87	>50 [a]	>50 [a]	5.9	Act [c]

[a] The values were determined in the reduction of 10 mM D-glucuronate (for AKR1A1) and 0.2 mM pyridine-3-aldehyde (for AKR1B1 and AKR1B10) in 0.1 M potassium phosphate, pH 7.4, containing 0.1 mM NADPH. The IC_{50} values for the AKR1C isoforms in the oxidative direction were assayed using 0.1 mM (for AKR1C1) and 1.0 mM *S*-(+)-1,2,3,4-tetrahydro-1-naphthol (for the other isoforms) as the substrates in the phosphate buffer containing 0.25 mM $NADP^+$.

[b] Less than 30% inhibition at the indicated concentration.

[c] Activation.